Evolution of the moments of multiplicity distributions

Radka Sochorová,[1] Boris Tomášik,[1,2] and Marcus Bleicher[3,4,5]
[1]*České vysoké učení technické v Praze, FJFI, Břehová 7, 11519 Praha 1, Czech Republic*
[2]*Univerzita Mateja Bela, Tajovského 40, 97401 Banská Bystrica, Slovakia*
[3]*Frankfurt Institute for Advanced Studies, Johann Wolfgang Goethe-Universität, Ruth-Moufang-Strasse 1, 60438 Frankfurt am Main, Germany*
[4]*Institut für Theoretische Physik, Johann Wolfgang Goethe-Universität, Max-von-Laue-Strasse 1, 60438 Frankfurt am Main, Germany*
[5]*GSI Helmholtz Center, Planckstrasse 1, 64291 Darmstadt, Germany*

(Received 2 October 2018; published 26 December 2018)

Measured moments of the multiplicity distribution for a given sort of particles are used in the literature for the determination of the phase transition parameters of hot QCD matter in ultrarelativistic heavy-ion collisions. We argue that the subsequent cooling in the hadronic phase, however, may drive the multiplicity distribution out of equilibrium. We use a master equation for the description of the evolution of the multiplicity distribution to demonstrate how the different moments depart away from their equilibrium values. If such moments were measured and interpreted as if they were equilibrated, one would obtain different apparent temperatures from different moments.

DOI: 10.1103/PhysRevC.98.064907

I. INTRODUCTION

Event-by-event fluctuations of the identified particle number observed in relativistic heavy-ion collisions carry the promise to exactly locate the state of the created QCD matter on the phase diagram at the time of hadron production [1–9]. The moments of the number distribution can be related to the susceptibilities which are expressed as derivatives of the partition function [6,10].

The susceptibilities are usually related to a conserved quantum number, e.g., the baryon number or strangeness. A large variety of susceptibilities are currently determined by lattice QCD methods up to the fourth order [11]. On the experimental side, moments of the net proton number distribution are also measured up to the fourth order [12–14]. Unfortunately, baryon number cannot be measured, as neutrons are not detected in many current experimental set-ups. Nevertheless, there are arguments that claim that the protons are a good proxy for the baryon number [15,16]. In real collision events, the observed proton number fluctuations, however, are also influenced by conservation laws [17,18]. In addition to net baryon number, the fluctuations of the number of strange particles are also measured [13,30].

From a comparison of experimental data to theoretical predictions of various moments of the multiplicity distribution, temperature, and chemical potentials of the created matter can be determined [19–21]. Note however, that the theoretical treatments—be it lattice QCD or the statistical model—use the grand-canonical formalism and assume equilibrium. The results obtained from such analyses show some disagreement between temperatures obtained from fitting the first moments (i.e., the yields) [22] and those obtained from fitting the higher moments [19].

Our study is directly motivated by such a mismatch. We qualitatively show that in an ensemble of expanding and cooling fireballs different moments of the number distribution may acquire values that seemingly do not correspond to each other if one tries to understand them with single temperature and chemical potential.

To clarify this point, let us stress that after hadronization inelastic collisions among hadrons still continue. Due to the decrease of the reaction rates they are unable to maintain the chemical composition so that it would fully respond to the changing temperature. In fact, the inelastic reactions alter the numbers of individual species and drive them off equilibrium. Our treatment thus goes beyond [23] where no inelastic collisions after chemical freeze-out were assumed.

Note further, that since we want to study the *fluctuations* of multiplicities, we inherently study an ensemble of fireballs and the time evolution of multiplicity distribution across the ensemble. As the distribution drops out of equilibrium, its moments may not be described by universal values of temperature and chemical potentials. This is the essence of the argument presented in this paper.

The appropriate tool for studying the evolution of multiplicity distributions is a master equation. Generally, in contrast to rate equations, master equations describe the evolution of the *whole discrete probability distribution* and not just the evolution of the mean values. The description is related to the microscopic processes which can change multiplicity of the studied kind of particles. In Sec. II we use a specific master equation which also respects exact $U(1)$ charge conservation [24] and derive the equilibrium values for the first four moments. Then, in Sec. III we look at how the formalism describes relaxation towards equilibrium. Phenomenologically relevant scenario of cooling is investigated in Sec. IV. Conclusions are presented in Sec. V.

II. THE MASTER EQUATION

For our study we shall investigate multiplicity distributions of species that conserve an Abelian charge, e.g., strangeness, and undergo the reaction $a_1a_2 \leftrightarrow b_1b_2$. Here, none of the involved species are identical to each other and it is understood that the b's carry the conserved charge while the a's do not. Also, it will be assumed that there is a sufficiently large pool of a's which is basically untouched by this chemical process.[1] In [24] the master equation for such a process has been derived which describes the time evolution of the multiplicity distribution P_n of species b. Here, P_n is the probability to have n pairs of those species. The master equation is formulated as

$$\frac{dP_n}{dt} = \frac{G}{V}\langle N_{a_1}\rangle\langle N_{a_2}\rangle[P_{n-1} - P_n] - \frac{L}{V}[n^2 P_n - (n+1)^2 P_{n+1}], \tag{1}$$

where V is the effective volume and G, L stand for the momentum-averaged cross section of the gain process ($a_1a_2 \to b_1b_2$) and the loss process ($b_1b_2 \to a_1a_2$), respectively,

$$G = \langle \sigma_G v\rangle,$$
$$L = \langle \sigma_L v\rangle .$$

We suppressed writing out explicitly that the P_n's are functions of time.

Equation (1) can be solved in order to obtain the evolution of all P_n's. If G, L, and V are constant, then it must describe the approach towards equilibrium. This is best studied if the master equation is put into dimensionless form

$$\frac{dP_n}{d\tau} = \varepsilon[P_{n-1} - P_n] - [n^2 P_n - (n+1)^2 P_{n+1}], \tag{2}$$

by scaling the time with relaxation time τ_0

$$\tau = \frac{t}{\tau_0}, \tag{3}$$

where

$$\tau_0 = V/L, \tag{4}$$
$$\varepsilon = \frac{G}{L}\langle N_{a_1}\rangle\langle N_{a_2}\rangle . \tag{5}$$

The equilibrium distribution can be then derived with the help of the generating function [24]

$$g(x,\tau) = \sum_{n=0}^{\infty} x^n P_n(\tau), \tag{6}$$

where x is an auxiliary variable.

[1]For too small numbers of a's, e.g., in collisions at lower energies within the RHIC Beam Energy Scan program, this assumption may not necessarily be warranted. This would lead to a modification of the master equation. We shall come to this point again in the discussion section.

The generating function is instrumental in calculating the factorial moments of the multiplicity distribution. It obeys the normalization condition

$$g(1,\tau) = \sum_{n=0}^{\infty} P_n(\tau) = 1, \tag{7}$$

and gives

$$g'(1,\tau) = \sum_{n=0}^{\infty} n P_n(\tau) = \langle n\rangle, \tag{8a}$$

$$g''(1,\tau) = \sum_{n=0}^{\infty} n(n-1) P_n(\tau) = \langle n(n-1)\rangle, \tag{8b}$$

$$g^{(3)}(1,\tau) = \sum_{n=0}^{\infty} n(n-1)(n-2) P_n(\tau) = \left\langle \frac{n!}{(n-3)!}\right\rangle, \tag{8c}$$

$$g^{(4)}(1,\tau) = \sum_{n=0}^{\infty} n(n-1)(n-2)(n-3) P_n(\tau) = \left\langle \frac{n!}{(n-4)!}\right\rangle. \tag{8d}$$

In order to find the equilibrium distribution, one derives from the master equation (2) the equation for the time evolution of $g(x,\tau)$ [24]

$$\frac{\partial g(x,\tau)}{\partial \tau} = (1-x)\left(x\frac{\partial^2 g}{\partial x^2} + \frac{\partial g}{\partial x} - \varepsilon g\right). \tag{9}$$

The equilibrium solution is found if the right-hand side is set equal to 0 [25]:

$$x\frac{\partial^2 g}{\partial x^2} + \frac{\partial g}{\partial x} - \varepsilon g = 0. \tag{10}$$

It reads

$$g_0(x) = \frac{I_0(2\sqrt{\varepsilon x})}{I_0(2\sqrt{\varepsilon})} \tag{11}$$

which fulfils the normalisation condition (7). Here, $I_0(x)$ is the modified Bessel function.

The equilibrium distribution is then

$$P_{n,eq} = \frac{\varepsilon^n}{I_0(2\sqrt{\varepsilon})(n!)^2}. \tag{12}$$

Through equations (8) the factorial moments can be calculated[2]:

$$\langle n\rangle_{eq} = \sqrt{\varepsilon}\frac{I_1(2\sqrt{\varepsilon})}{I_0(2\sqrt{\varepsilon})}, \tag{13a}$$

$$\langle n(n-1)\rangle_{eq} = -\frac{1}{2}\sqrt{\varepsilon}\frac{I_1(2\sqrt{\varepsilon})}{I_0(2\sqrt{\varepsilon})} + \frac{1}{2}\varepsilon\frac{I_2(2\sqrt{\varepsilon}) + I_0(2\sqrt{\varepsilon})}{I_1(2\sqrt{\varepsilon})}, \tag{13b}$$

[2]The first and second factorial moments have been calculated in [24,25].

$$\left\langle \frac{n!}{(n-3)!} \right\rangle_{eq} = \frac{3}{4}\sqrt{\varepsilon}\frac{I_1(2\sqrt{\varepsilon})}{I_0(2\sqrt{\varepsilon})} - \frac{3}{4}\varepsilon\left(1+\frac{I_2(2\sqrt{\varepsilon})}{I_0(2\sqrt{\varepsilon})}\right) + \frac{1}{4}\varepsilon^{3/2}\frac{I_3(2\sqrt{\varepsilon})+3I_1(2\sqrt{\varepsilon})}{I_0(2\sqrt{\varepsilon})}, \quad (13c)$$

$$\left\langle \frac{n!}{(n-4)!} \right\rangle_{eq} = -\frac{15}{8}\sqrt{\varepsilon}\frac{I_1(2\sqrt{\varepsilon})}{I_0(2\sqrt{\varepsilon})} + \frac{15}{8}\varepsilon\left(\frac{I_2(2\sqrt{\varepsilon})}{I_0(2\sqrt{\varepsilon})}+1\right) - \frac{3}{4}\varepsilon^{3/2}\frac{3I_1(2\sqrt{\varepsilon})+I_3(2\sqrt{\varepsilon})}{I_0(2\sqrt{\varepsilon})} + \frac{1}{8}\varepsilon^2\left(3+\frac{4I_2(2\sqrt{\varepsilon})+I_4(2\sqrt{\varepsilon})}{I_0(2\sqrt{\varepsilon})}\right). \quad (13d)$$

These analytical expressions for equilibrium values of the factorial moments allow us to assess separately the departure from equilibrium for different orders.

Other characteristics of the distribution, like the central moments, cumulants, skewness, or kurtosis, etc., can be calculated by combinations of these factorial moments.

To scale out the total number of particles, we shall also study the scaled factorial moments

$$F_2 = \frac{\langle n(n-1)\rangle}{\langle n\rangle^2}, \quad (14a)$$

$$F_3 = \frac{\left\langle \frac{n!}{(n-3)!} \right\rangle}{\langle n\rangle^3}, \quad (14b)$$

$$F_4 = \frac{\left\langle \frac{n!}{(n-4)!} \right\rangle}{\langle n\rangle^4}. \quad (14c)$$

III. THERMALIZATION

The goal is to study why and how different moments of multiplicity distribution may indicate different temperatures. We therefore first study how the various moments relax towards their equilibrium values in an environment with constant temperature.

If the temperature and cross section are fixed, then the only time scale in the problem does not change and we can use Eq. (2) for the evolution of the multiplicity distribution.

The presented results have been obtained from a simulation with binomial initial conditions:

$$P_0(\tau=0) = 1-n_0, \quad (15a)$$

$$P_1(\tau=0) = n_0, \quad (15b)$$

$$P_i(\tau=0) = 0 \qquad \text{for } i>1, \quad (15c)$$

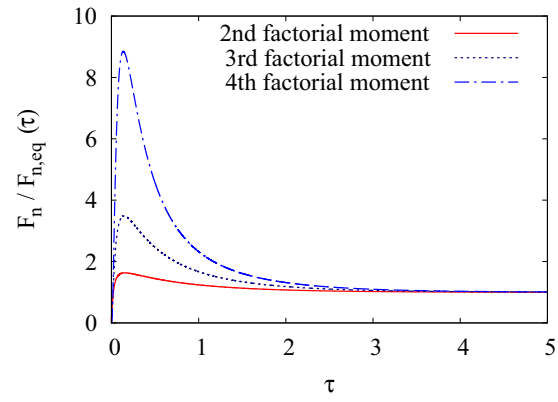

FIG. 1. Relaxation of the scaled factorial moments as functions of dimensionless time τ. Binomial initial conditions with $\varepsilon = 0.1$ and $n_0 = 0.005$ have been used.

where

$$n_0 = \langle n\rangle(\tau=0)$$

is the mean multiplicity of species b at the beginning.

The evolution of second to fourth scaled factorial moments divided by their equilibrium values [from Eqs. (13)] is shown in Fig. 1.

The value of the parameter ε has been set to 0.1 and the initial mean to $n_0 = 0.005$. Note that we have obtained qualitatively similar results also with other sets of parameters. Initial conditions which follow the Poisson distribution lead to similar rates of relaxation although the initial part of the dependence is different.

The higher moments are more sensitive to the shape of the distribution function beyond just its width. Thus one might have anticipated, that they more easily depart from their equilibrium values and it might take longer time for them to reach equilibrium. While the first statement holds, the second assertion is not fulfilled. Higher moments indeed depart further away from the equilibrium values in a nonequilibrium situation. However, they actually relax in the same time as the lower moments.

IV. NONEQUILIBRIUM COOLING

The fireballs produced in ultrarelativistic heavy-ion collisions cool down rapidly. It is therefore expected that the number distribution departs from equilibrium. In our simulation we shall assume that the system is equilibrated at the hadronization temperature $T = 165$ MeV. Due to subsequent expansion, the temperature decreases quickly. For a system that stays in equilibrium a lower temperature would correspond to a different multiplicity distribution. However, a prerequisite to maintain equilibrium is to ensure that the creation and annihilation reactions are capable of running at rates comparable to the expansion rate, otherwise the equilibrium will be lost. We explore what this means for the values of the moments.

To set up the environment, we shall assume Björken one-dimensional boost invariant expansion, where the proper

volume grows linearly

$$V(t) = V_0 \frac{t}{t_0} \tag{16}$$

and the temperature drops according to

$$T^3(t) = T_0^3 \frac{t_0}{t}\,. \tag{17}$$

In the calculations we have set $V_0 = 125\,\mathrm{fm}^3$. The temperature will start at the value of 165 MeV and drop down to 100 MeV. The latter is typically the temperature of the kinetic freeze-out.[3] Motivated by the femtoscopic measurements we set the final time to 10 fm/c. This then leads to $t_0 = 2.2\,\mathrm{fm}/c$.

For the actual calculation we must also choose the particular inelastic process. Processes with too small cross-sections will not be able to change anything on the multiplicity distributions while those with very large cross sections will practically simultaneously adjust them to the decreasing temperature. The relevant time scale is the relaxation time, given in Eq. (4). The interesting regime is when the relaxation time is comparable to the inverse expansion rate and the lifetime of the fireball.

We consider the reaction $\pi^+ n \leftrightarrow K^+\Lambda$. For the moment we shall use a parametrization of the cross section [29]

$$\sigma_{\pi N}^{\Lambda K} = \begin{cases} 0\,\mathrm{fm}^2 & \sqrt{s} < \sqrt{s_0} \\ \frac{0.090(\sqrt{s}-\sqrt{s_0})}{0.091}\,\mathrm{fm}^2 & \sqrt{s_0} \leqslant \sqrt{s} < \sqrt{s_0} + 0.09\,\mathrm{GeV}, \\ \frac{0.0090}{\sqrt{s}-\sqrt{s_0}}\,\mathrm{fm}^2 & \sqrt{s} \geqslant \sqrt{s_0} + 0.09\,\mathrm{GeV} \end{cases} \tag{18}$$

where $\sqrt{s_0}$ is the threshold energy of the reaction and the energies are given in GeV. Unfortunately, the flux-averaged gain and loss terms with this cross section are too small and lead to too low reaction rates. In order to proceed with qualitative studies, the cross section has been scaled up by hand so that the relaxation time is a few fm/c. Note that the gain term [Eq. (2)] of this reaction is small due to the rather high threshold, which is about 530 MeV above the masses of the incoming particles, while the temperature is lower than 165 MeV. This indicates that the reaction rate might increase considerably if the threshold is lowered, for example through the decrease of the hyperon mass in baryonic matter. This possibility will be investigated below.

In Fig. 2 we show how the relaxation time changes as the fireball expands and cools down. The relaxation time decreases with increasing temperature and/or with increasing cross-section. We have performed calculations with all scales of the cross sections indicated in Fig. 2.

First, we present in Fig. 3 the evolution of the scaled factorial moments. Due to decreasing temperature the moments change, but the reaction rate is too low to keep them in equilibrium. As observed above, the relative departure from equilibrium is larger for moments of higher order.

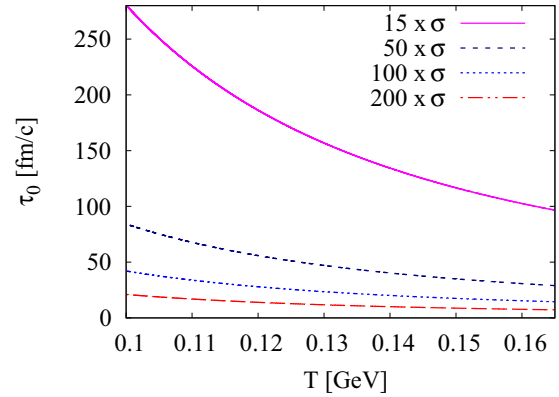

FIG. 2. Dependence of the relaxation time on temperature for scaled cross sections. There are 15 pions and 10 neutrons and the initial volume of 125 fm^3 expands according to Eq. (16).

We can now demonstrate the potential danger in case of extraction of the freeze-out temperature from the different moments. Suppose that the system breaks up at final (kinetic) temperature of 100 MeV, i.e., the moments assume their final values at this point. How does one usually infer the temperature from such a measurement? One *assumes thermalization*. The moments of a thermalized system would have evolved along the thin curves in Fig. 3. So the assumption of thermalization means that one assumes that the thin lines provide the correct description of the moments. However, in reality the moments evolved along the thick lines in Fig. 3. The arrows in that figure show how the apparent freeze-out temperature would be extracted. The actual observed final value of a thick line is projected horizontally on the corresponding thin line (Fig. 3) and the apparent temperature is read off from the projected point. We can see that such a procedure can lead to different values of apparent temperature if different moments are used.

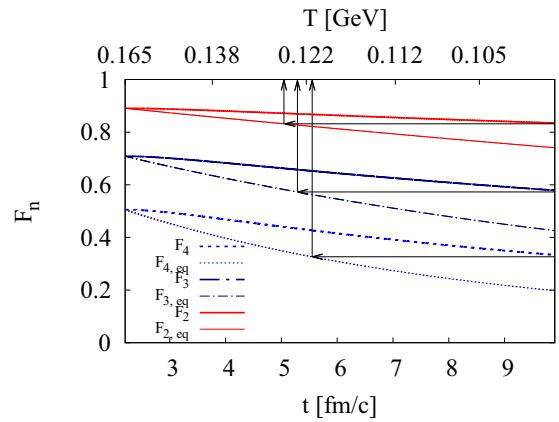

FIG. 3. Evolution of the scaled factorial moments. Thick lines: values calculated through the master equation (1), thin lines: equilibrium values calculated from relations (13).

[3]There is no general agreement in the literature concerning the kinetic freeze-out temperature. While fits with the blast-wave model without resonances yield temperatures around 120 MeV for collisions at RHIC [26], fits with resonance decays included give temperatures of 100 MeV [27] and lower [28], depending on the details of the model.

Factorial moments are usually not measured. More common are the central moments

$$\mu_1 = \langle n \rangle = M, \tag{19a}$$

$$\mu_2 = \langle n^2 \rangle - \langle n \rangle^2 = \sigma^2, \tag{19b}$$

$$\mu_3 = \langle (n - \langle n \rangle)^3 \rangle, \tag{19c}$$

$$\mu_4 = \langle (n - \langle n \rangle)^4 \rangle, \tag{19d}$$

or their derived characteristics: the skewness

$$S = \frac{\mu_3}{\mu_2^{3/2}} \tag{20}$$

and the kurtosis

$$\kappa = \frac{\mu_4}{\mu_2^2} - 3. \tag{21}$$

Their equilibrium values can all be calculated from proper combinations of the factorial moments and using the equilibrium values derived in Eqs. (13).

We plot the evolution of central moments for different scales of the cross section in Fig. 4. As expected, larger cross sections maintain the calculated values closer to the equilibrium ones. Also, moments of different orders generally indicate different apparent freeze-out temperatures, if interpreted as equilibrium values.

The skewness and kurtosis are even more interesting (Fig. 5). Their equilibrium values grow as the temperature decreases. This is not true, however, for the numerically calculated curves. Only those with larger cross sections do increase, while those with smaller cross-sections decrease. Clearly, the apparent freeze-out temperature could only be determined from those numerically calculated curves, which increase with the temperature.

For the sake of completeness, we also look at the volume-independent ratios which are often measured due to their easier comparison with theory. These are

$$R_{32} = \frac{\mu_3}{\mu_2} = S\sigma, \tag{22a}$$

$$R_{42} = \frac{\mu_4}{\mu_2} - 3\mu_2 = \kappa\sigma^2, \tag{22b}$$

$$R_{12} = \frac{\mu_1}{\mu_2} = \frac{M}{\sigma^2}, \tag{22c}$$

$$R_{31} = \frac{\mu_3}{\mu_1} = \frac{S\sigma^3}{M}. \tag{22d}$$

The evolution of these ratios for different cross sections, together with the equilibrium values at actual temperatures, are presented in Fig. 6. We find that some of the ratios, notably R_{12} and R_{31}, evolve qualitatively differently from the equilibrium value for any value of the cross section.

In summary, simple factorial and central moments behave so that for larger cross section we see how they approach the equilibrium behavior. However, when they are combined into more complicated observables, like skewness, kurtosis, or the volume-independent ratios, the departure from the equilibrium is considerable and even qualitative. We conclude that these observables are actually very fragile with respect to nonequilibrium chemical evolution and very easily depart from values which can be interpreted in terms of equilibrium distribution.

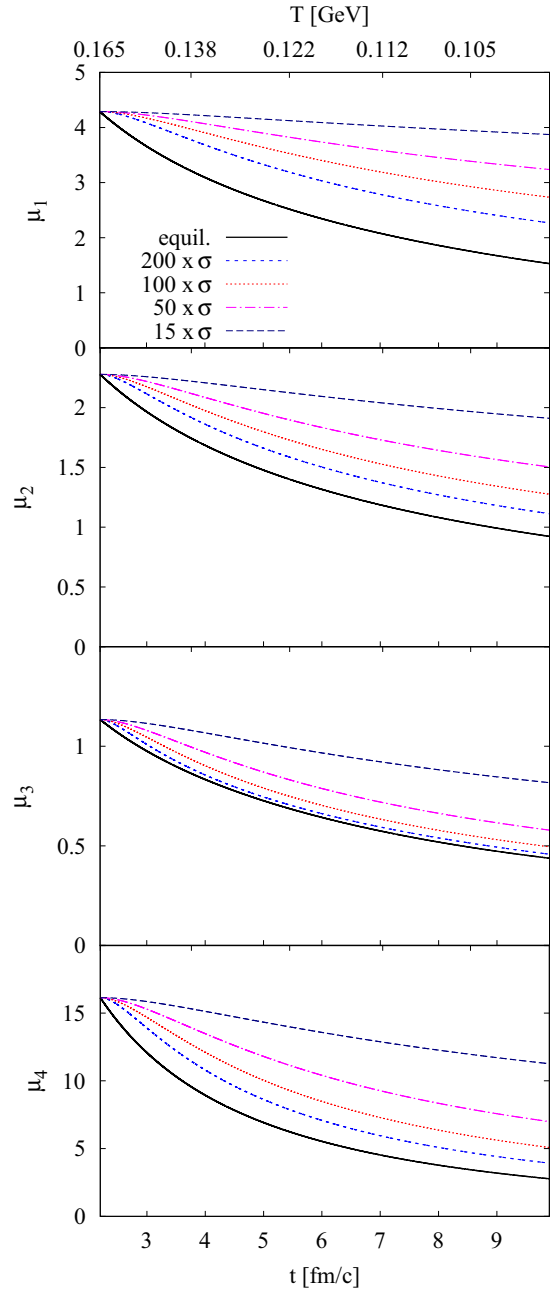

FIG. 4. Evolution of the first four central moments (from top to bottom). Different curves on the same panel show results for different cross sections. Solid lines show the equilibrium values.

The previous studies presented in this work have been performed with cross sections that were scaled unrealistically high for the given reaction. The aim was to use this reaction as a proxy for any other processes which can produce the b species. This is acceptable, because our conclusions from the study are only qualitative.

Nevertheless, it is also unrealistic to assume that the masses and cross sections in hot and dense baryonic matter keep

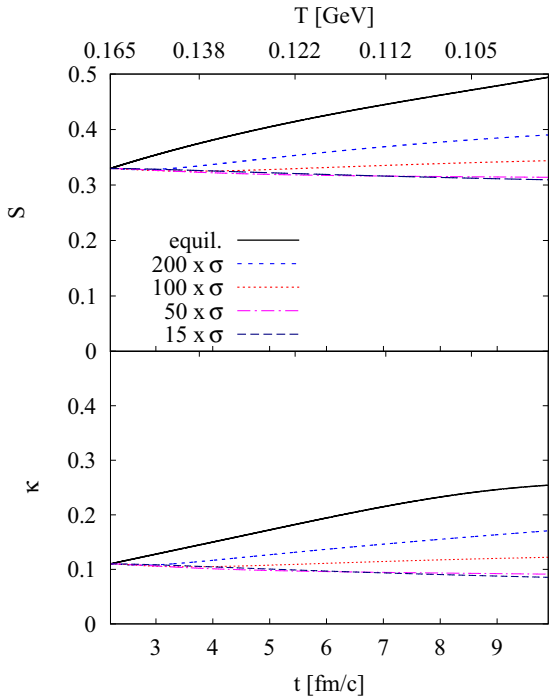

FIG. 5. Evolution of the skewness (upper panel) and the kurtosis (lower panel). Different curves on the same panel show results for different cross sections. Solid lines show the equilibrium values.

their vacuum values. Moreover, by lowering the mass of the hyperon, also the threshold for the reaction is lowered, and its rate may grow due to the increase of the available phase space. We shall assume rather extreme and simplified dependence of the hyperon mass on baryon density

$$m_\Lambda(\rho_B) = \frac{\rho_0 - \rho_B}{\rho_0} m_{\Lambda 0} + \frac{\rho_B}{\rho_0} m_p \tag{23}$$

so that the hyperon mass becomes identical to that of the proton at the highest baryon density ρ_0 at which our calculation starts, and returns to the vacuum value $m_{\Lambda 0}$ if baryon density vanishes. The cross section in Eq. (18) is modified by replacing the threshold $\sqrt{s_0}$ by the new value $m_K + m_\Lambda(\rho_B)$.

Selected results from the scenario with density-dependent mass of the hyperon are plotted in Fig. 7. The rate of the reaction is clearly too small to keep the system in chemical equilibrium. However, thanks to the increase of the cross section at the highest baryon densities the system is clearly driven away from the state which is present at the initial temperature of 165 MeV. All central moments are slightly decreasing, because the multiplicity of strange particles goes down. The hierarchy of the departure from the initial value is such that it grows with the order of the moment. Only slight changes are seen for the skewness and the kurtosis and somewhat stronger departure is observed for the volume independent ratios $S\sigma$ and $\kappa\sigma^2$. Interestingly, for the latter even the equilibrium values seem not to change much, although this is rather accidental.

Nevertheless, in realistic fireballs there are other channels that can change the numbers of kaons and/or λs and so we have to expect a variation of moments yet larger than indicated

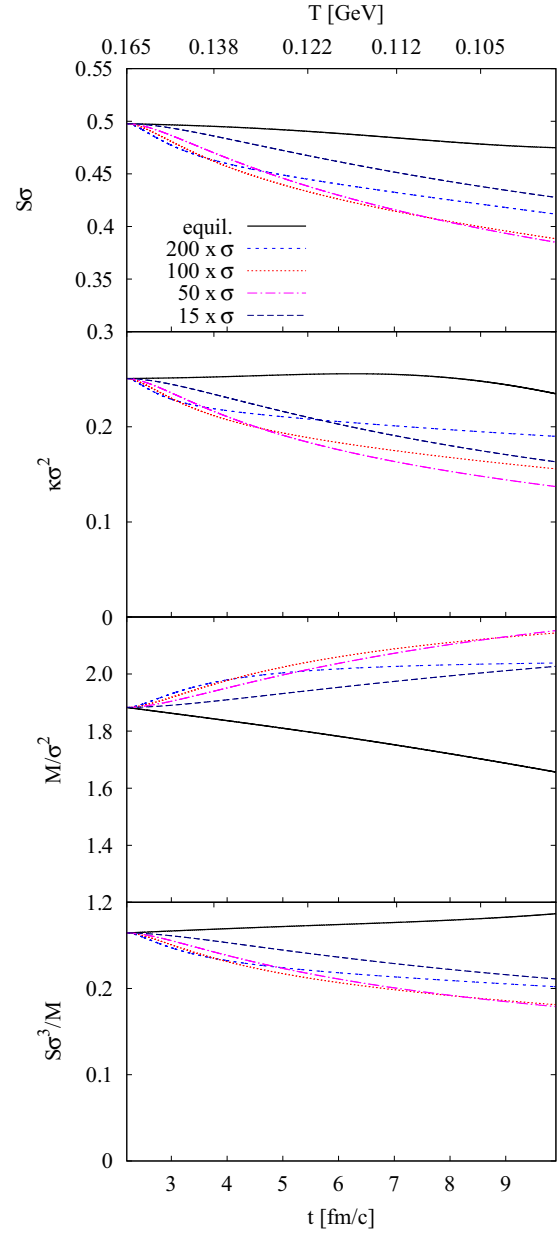

FIG. 6. Evolution of the volume-independent ratios. Different curves on the same panel show results for different cross sections. Solid lines show the equilibrium values.

by these calculations. We conclude that with a realistic scenario the evolution of the composition of the fireball may be capable of influencing the fluctuations of the particle number distribution to a measurable extent.

V. DISCUSSION

In this work, we have explored one of the effects that may influence the higher moments of the multiplicity distribution of identified particles. In general, if hadronization is followed by a rescattering phase, the multiplicity distribution may become off-equilibrium. This means that not only the average

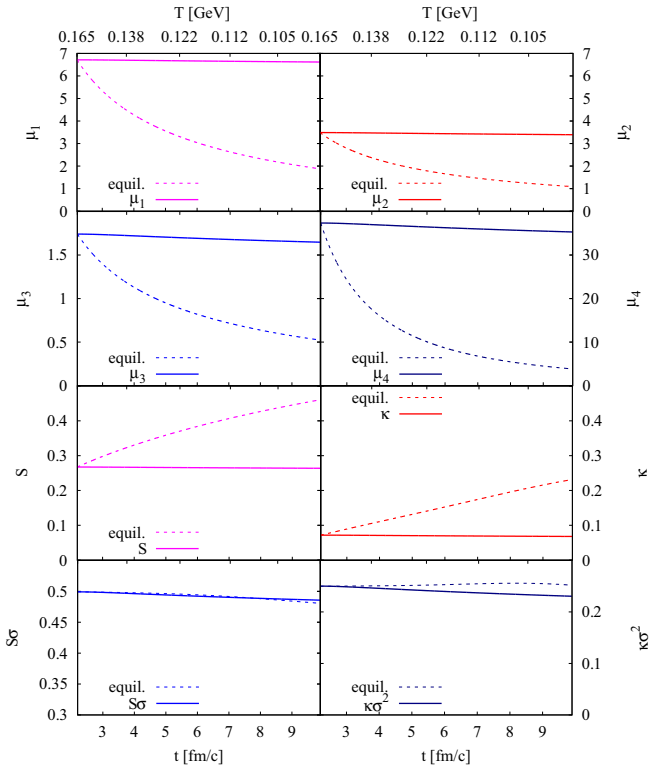

FIG. 7. Central moments, skewness, kurtosis, and volume-independent ratios $S\sigma$ and $\kappa\sigma^2$ for the scenario with density-dependent mass of Λ. Thick solid lines: numerically calculated evolution; thin dotted lines: equilibrium values at the given temperature.

number of particles may change, but also the higher moments depart from their equilibrium values.

The master equation (1) adopted from [24] and used here is suitable for the description of single reaction channel which produces a $U(1)$ conserved charge. It can be used for the studies of rare species, like charm or bottom. Of course, the measurement of moments of their multiplicity distribution is a challenge which is very hard to overcome.

We have applied the formalism to one reaction channel which produces strangeness, and we have studied the fluctuations of strange particles. The higher moments of kaon multiplicity distribution have been measured within the BNL Relativistic Heavy Ion Collider (RHIC) Beam Energy Scan program by the STAR collaboration [30]. We have made an attempt to apply our calculations to the interpretation of those data. However, this actually revealed that our calculation is only a part of a more complex description. Firstly, there are certainly other channels that influence the number distribution of strange particles. Secondly—and probably more importantly—we do not know the initial conditions for the evolution.

Let us also come to the point raised in the introduction of the master equation: what would happen if we cannot replace the numbers of a species just by their averages. The master equation would slightly change, but the general feature of our results remains: the different moments of the number distribution depart from their equilibrium values, and higher moments do that more than the lower moments.

As a side project we have also looked at the isospin-randomising reactions which turn protons into neutrons and vice versa. Such reactions have large cross sections and no threshold. Hence, they are very frequent. Consequently, we observed that the moments of multiplicity distribution of protons do not change even with decreasing temperature if they are started in equilibrium. This is in line with the findings of [15,16] and it is a good news for the measurements of proton number fluctuations, which try to relate the measured moments to the baryon number susceptibilities of the matter at the point of hadronization.

It appears as an interesting question, whether the formalism of master equations can be also used for the description of the deconfined phase of the collision. Recall that the evolution is interesting if the reaction rates are comparable to the rate of temperature decrease. This rules out the description of light quarks, which are produced and destroyed too easily. It also disqualifies the description of charm and bottom, which are too heavy to be produced in the quark-gluon plasma. What remains is the production of strange quarks, which might be interesting in a regime where QGP is produced, yet strangeness is not chemically equilibrated. The treatment, however might not be easy. Firstly, a different master equation must be derived which takes into account production from $q\bar{q}$ annihilations as well as gg reactions. Secondly, it is expected that in this window of collision energies the system may spent an important portion of its time at temperatures just above the hadronization. There, it is strongly coupled, interactions are nonperturbative, and the microscopic description with quarks and gluons becomes complicated [31].

Coming back to hadronic reactions investigated in this paper, we conclude that inelastic reactions in a system with decreasing temperature may alter the individual moments of the multiplicity distribution differently. Importantly, they can push the moments away from their values at the beginning of cooling. Such moments are being measured with the hope that their precise values will help us to better pinpoint the position of the strongly interacting matter on the phase diagram. Therefore, a word of caution must be raised that the values of the moments at hadronization may be severely altered in subsequent evolution. Master equations are effective tools for the investigation of these effects.

ACKNOWLEDGMENTS

We thank E.E. Kolomeitsev, L. Lafférs, and M. Šumbera for enlightening discussions. This work was supported by Grant No. 17-04505S of the Czech Science Foundation (GAČR). This work was supported by collaboration grant in framework of the German-Slovak PPP programme and the COST Action CA15213 THOR. This work was supported by HIC for FAIR within the Hessian LOEWE initiative. B.T. acknowledges support by VEGA 1/0348/18 (Slovakia).

[1] M. Asakawa, U. Heinz, and B. Müller, Phys. Rev. Lett. **85**, 2072 (2000).
[2] Y. Hatta and M. A. Stephanov, Phys. Rev. Lett. **91**, 102003 (2003); **91**, 129901(E) (2003).
[3] V. Koch, A. Majumder, and J. Randrup, Phys. Rev. Lett. **95**, 182301 (2005).
[4] S. Ejiri, F. Karsch, and K. Redlich, Phys. Lett. B **633**, 275 (2006).
[5] B. Stokic, B. Friman, and K. Redlich, Phys. Lett. B **673**, 192 (2009).
[6] C. Athanasiou, K. Rajagopal, and M. Stephanov, Phys. Rev. D **82**, 074008 (2010).
[7] R. V. Gavai and S. Gupta, Phys. Lett. B **696**, 459 (2011).
[8] M. A. Stephanov, Phys. Rev. Lett. **107**, 052301 (2011).
[9] S. Gupta, X. Luo, B. Mohanty, H. G. Ritter, and N. Xu, Science **332**, 1525 (2011).
[10] M. A. Stephanov, Phys. Rev. Lett. **102**, 032301 (2009).
[11] A. Bazavov, H.-T. Ding, P. Hegde, O. Kaczmarek, F. Karsch, E. Laermann, S. Mukherjee, H. Ohno, P. Petreczky, E. Rinaldi, H. Sandmeyer, C. Schmidt, C. Schroeder, S. Sharma, W. Soeldner, R. A. Soltz, P. Steinbrecher, and P. M. Vranas (HotQCD Collaboration), Phys. Rev. D **96**, 074510 (2017).
[12] L. Adamczyk *et al.* (STAR Collaboration), Phys. Rev. Lett. **112**, 032302 (2014).
[13] A. Ohlson (ALICE Collaboration), PoS **CPOD2017**, 031 (2018).
[14] M. Szala *et al.* (HADES Collaboration), J. Phys.: Conf. Ser. **1024**, 012024 (2018).
[15] M. Kitazawa and M. Asakawa, Phys. Rev. C **85**, 021901(R) (2012).
[16] M. Kitazawa and M. Asakawa, Phys. Rev. C **86**, 024904 (2012); **86**, 069902(E) (2012).
[17] A. Bzdak, V. Koch, and V. Skokov, Phys. Rev. C **87**, 014901 (2013).
[18] P. Braun-Munzinger, A. Rustamov, and J. Stachel, Nucl. Phys. A **960**, 114 (2017).
[19] P. Alba, W. Alberico, R. Bellwied, M. Bluhm, V. Mantovani Sarti, M. Nahrgang, and C. Ratti, Phys. Lett. B **738**, 305 (2014).
[20] R. Bellwied, J. Noronha-Hostler, P. Parotto, I. Portillo Vazquez, C. Ratti, and J. M. Stafford, arXiv:1805.00088 [hep-ph].
[21] M. Bluhm and M. Nahrgang, arXiv:1806.04499 [nucl-th].
[22] A. Andronic, P. Braun-Munzinger, K. Redlich, and J. Stachel, Nature **561**, 321 (2018).
[23] M. A. Stephanov, Phys. Rev. D **81**, 054012 (2010).
[24] C. M. Ko, V. Koch, Z. W. Lin, K. Redlich, M. A. Stephanov, and X. N. Wang, Phys. Rev. Lett. **86**, 5438 (2001).
[25] S. Jeon, V. Koch, K. Redlich, and X. N. Wang, Nucl. Phys. A **697**, 546 (2002).
[26] L. Adamczyk *et al.* (STAR Collaboration), Phys. Rev. C **96**, 044904 (2017).
[27] I. Melo and B. Tomášik (unpublished).
[28] S. P. Rode, P. P. Bhaduri, A. Jaiswal, and A. Roy, Phys. Rev. C **98**, 024907 (2018).
[29] J. Cugnon and R. M. Lombard, Nucl. Phys. A **422**, 635 (1984).
[30] L. Adamczyk *et al.* (STAR Collaboration), Phys. Lett. B **785**, 551 (2018).
[31] A. Peshier and W. Cassing, Phys. Rev. Lett. **94**, 172301 (2005).